3-D diffusion-reaction model for hexagonal surface layers

Po-Nan Li[*]

Department of Electrical Engineering, Stanford University

(Dated: June 28, 2018)

Abstract

A diffusion-reaction numerical solver capable of studying the ion transport in a hexagonal structure is implemented. The simulation is 3-dimensional but computationally efficient by taking advantage of the cylindrical coordinate system. Further computation reduction is done by reducing the computation domain six-fold. The implemented solver is utilized to study a simplified model of archaeal surface layer, which is a charged hexagonal sheet with an opening.

----

[*] liponan@stanford.edu

I. INTRODUCTION

Surface layers (S-layers) are proteinous lattice that are possessed by most of archaea and some of the bacteria as their outermost envelope [1, 2]. Although structurally diverse, S-layers' functions are essentially similar: provide mechanical support and act as a particle sieve to protect the cell. While the surface topography of the S-layer has been extensively studied, little is known about the how does the S-slayer serve as a selective barrier. Specifically, it is well accepted that the pores on the surface would allow or reject specific particles to enter the cell. However, the mechanism of such sieving remains elusive, e.g. how would the pore prohibits the entry of particles that are much smaller than its opening.

Methanosarcina acetivorans, for example, possess an S-layer that is consisting of repeating hexagonal tiles [3]. It is reported that the S-layer of M. acetivorans has a funnel-like structure, and a center-to-center distance of 12 nm between the pores, whose opening is roughly 1.3 nm. Arbing *et al.* find that S-layer of M. acetivorans is negatively charged, which could be critical for its function.

Ammonia oxdizing archaea (AOA), a major player of the global ammonia cycling, is another instance of cell that has hexagonal surface layer lattice. An unpublished manuscript reports that the S-layer of AOA also has pores that have center-to-center distance of 22 nm and shows the evidence that S-layer is negatively charged [4]. Some researchers have hypothesized that AOA's S-layer plays a role of facilitating the ammonium oxidization, for which an enzyme, namely ammonia monooxygenase (AMO), is responsible [5].

In this project, a continuum diffusion-reaction model is built to study the ion transport near the S-layer of AOA. In particular, special boundary condition (BC) setting is designed to enable the realization of six-fold symmetry on top of cylindrical coordinate to reduce computation, as shown in FIG. 1(a) and will be discussed in the following sections. The simulation model also includes a reaction site, where NH_4^+ ions will be consumed, and a surface layer with negative surface charges and a pore, as shown in FIG. 1(b).
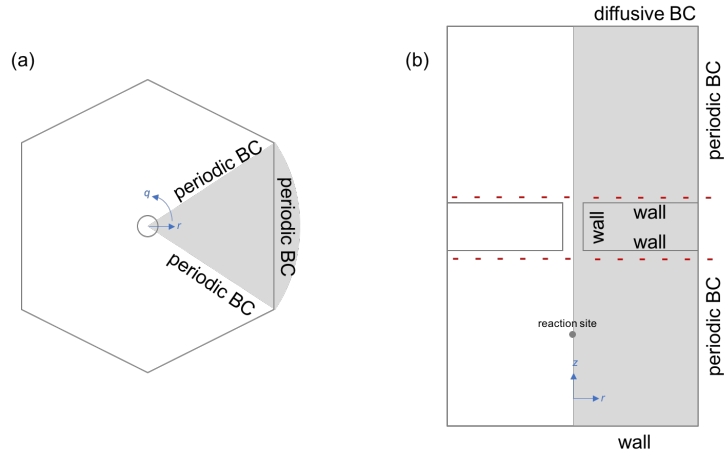
FIG. 1. Schematic of the simulation domain that will be studied in this project, which is a hexagonal prism. (a) Top view of the domain. Thanks to the six-fold symmetry, only a 1/6 "pizza slice," as indicated by the shaded area, needs to be calculated. (b) Side view of the domain. An S-layer with a pore is placed in the center of the domain. Negative charges are uniformly distributed on the two sides of the S-layer. A voxel-large reaction site is placed at the center of the intracelluar space. Shaded area indicates the area that will actually be computed, while the other half is simply the flipped version of the shaded area.

II. THEORY

A. Fick's Laws

Fick's first law of diffusion is an elegant way to describe the diffusion along a space coordinate given a diffusion constant and a gradient of concentration:

$$J = -D\frac{dc}{dx} \tag{1}$$

where J is the flux along the x direction, D is the diffusion constant and c is the concentration profile and a function of space x. To further describe the diffusion behavior as a function of time, one might use the following partial differential equation

$$\frac{\partial c}{\partial t} = D\frac{\partial^2 c}{\partial x^2}, \tag{2}$$

which is known as Fick's second law. To numerically solve the concentration profile as a function of time and space, one might discretize a 2-D model into grid cells, and re-write

eq. (2) as

$$\frac{c(i,j)^{(t+1)} - c(i,j)^t}{\Delta t} = D\frac{c(i+1,j)^{(t)} - c(i-1,j)^{(t)}}{2\Delta x} + D\frac{c(i,j+1)^{(t)} - c(i,j-1)^{(t)}}{2\Delta y}, \quad (3)$$

where Δx and Δy are the grid size along the x and y direction, respectively. Note here the central difference is used to represent the second-order finite difference. Finally eq. (1) is plugged in and (3) is re-arranged, obtaining

$$
\begin{aligned}
c(i,j)^{(t+1)} =& c(i,j)^t - \Delta t \left[\frac{\partial J_x}{\partial x} + \frac{\partial J_y}{\partial y} \right] \\
\frac{\partial J_x}{\partial x} =& \frac{J_x(i+\frac{1}{2},j) - J_x(i-\frac{1}{2},j)}{\Delta x} \\
\frac{\partial J_y}{\partial y} =& \frac{J_y(i,j+\frac{1}{2}) - J_y(i,j-\frac{1}{2})}{\Delta y}
\end{aligned}
\quad (4)
$$

where

$$
\begin{aligned}
J_x(i+\tfrac{1}{2},j) =& -D\frac{c(i+1,j) - c(i,j)}{\Delta x} \\
J_y(i,j+\tfrac{1}{2}) =& -D\frac{c(i,j+1) - c(i,j)}{\Delta y}
\end{aligned}
\quad (5)
$$

are the finite difference version of (1). Note here here a half-step ($\frac{1}{2}$) is used to indicate the fact that the grid cells of J_x and J_y are not aligned with that of c; instead, there is a $\frac{1}{2}$ offset along the x or y axis, as shown in FIG. 2(a). Given proper initial condition (IC) and boundary condition (BC) setting, one might update equations (4) and (5) alternately to build a numerical diffusion solver.

While (1) is for one-dimensional, it is not difficult to write down the Fick's first law equation in the cylindrical coordinates:

$$\mathbf{J} = -D\frac{\partial c}{\partial r} - D\frac{1}{r}\frac{\partial c}{\partial \phi} - D\frac{\partial c}{\partial z}, \quad (6)$$

which has discrete form

$$
\begin{aligned}
J_r(i+\tfrac{1}{2},j,k) =& -D\frac{c(i+1,j,k) - c(i,j,k)}{\Delta r} \\
J_q(i,j+\tfrac{1}{2},k) =& -\frac{D}{r}\frac{c(i,j+1,k) - c(i,j,k)}{\Delta q} \\
J_z(i,j,k+\tfrac{1}{2}) =& -D\frac{c(i,j,k+1) - c(i,j,k)}{\Delta z},
\end{aligned}
\quad (7)
$$

where q is the notation for the discrete angular coordinate. Based on the cylindrical coordinate form of the Lalpace operator, the updating equation of the concentration can be

4

formulated as

$$\frac{\partial c}{\partial t} = D\nabla^2 c = D\left[\frac{1}{r}\frac{\partial}{\partial r}\left(r\frac{\partial c}{\partial r}\right) + \frac{1}{r^2}\frac{\partial^2 c}{\partial \phi^2} + \frac{\partial^2 c}{\partial z^2}\right], \tag{8}$$

which has discrete form:

$$c(i,j,k)^{(t+1)} = c(i,j,k)^{(t)} - \Delta t\left[\frac{1}{r}\frac{\partial}{\partial r}(rJ_r) + \frac{1}{r}\frac{\partial}{\partial q}(J_q) + \frac{\partial}{\partial z}(J_z)\right], \tag{9}$$

where J_q, J_q and J_z are already introduced in (7).

B.   Poisson-Nernst-Planck equations

In some cases, it is desirable to simulate the diffusion behavior of ions, i.e. charged particles, which emit and are subject to the influence of electric-fields. It is not difficult to formulate a Poisson equation given the concentration c_k and valence charge c_k of the mobile ion spices k:

$$-\nabla \cdot (\epsilon\nabla\phi) = 4\pi\rho_f + \sum_k 4\pi z_k c_k, \tag{10}$$

where ρ_f denotes the distribution of fixed charges. To incorporate the Poisson equation into the updating equations, here I use an alternative, equivalent version [6], which represents the Poisson equation as electric-field as a function of time

$$\frac{\partial \mathbf{E}}{\partial t} = -\frac{N_A e}{\epsilon}\sum_k z_k \mathbf{J_k}. \tag{11}$$

With the above equation, the updating equation of flux $\mathbf{J}$ can be formulated as

$$\begin{aligned} J_x &= -D\left[\nabla_x c\right] + \frac{N_A e}{RT}DzcE_x \\ J_y &= -D\left[\nabla_y c\right] + \frac{N_A e}{RT}DzcE_y, \end{aligned} \tag{12}$$

where T denotes the temperature, R is the gas constant, N_A is Avogadro's number, e denotes the elementary charge, and z denote the valance charge of the ion.

Finally, one might add a reaction term $R(c)$, which is a function of concentration and space and write

$$\begin{aligned} \frac{\partial c}{\partial t} &= -\nabla \cdot \mathbf{J} + R(c) \\ &= -\nabla \cdot \left[-D\nabla c + \frac{N_A e Dz}{RT}c\mathbf{E}\right] - \frac{k_{rec}}{k_M}\frac{c}{N_A(\Delta x)^3}\delta(x - x_{rec}), \end{aligned} \tag{13}$$

5

which is known as a Poisson-Nernst-Planck (PNP) equation with a reaction term, where $x_r ec$ is the position of the reaction site. Again, (13) is just the one-dimensional case which is good for illustration. To derive a three-dimensional and discrete version, one might modify (9), obtaining

$$
\begin{aligned}
c(i,j,k)^{(t+1)} =& c(i,j,k)^{(t)} \\
& - \Delta t \left[\frac{1}{r}\frac{\partial}{\partial r}(rJ_r) + \frac{1}{r}\frac{\partial}{\partial q}(J_q) + \frac{\partial}{\partial z}(J_z) \right] \\
& - \Delta t \frac{k_{rec}}{k_M} \frac{c(i,j,k)^{(t)}}{N_A \pi (\Delta r)^2 \Delta z} \delta(i - i_{rec}, j - j_{rec}, k - k_{rec}),
\end{aligned}
\tag{14}
$$

where

$$
\begin{aligned}
J_r(i+\tfrac{1}{2}, j, k) =& -D\frac{c(i+1,j,k) - c(i,j,k)}{\Delta r} + \frac{N_A e}{RT} DzE_r \frac{c(i+1,j,k) + c(i,j,k)}{2} \\
J_q(i, j+\tfrac{1}{2}, k) =& -\frac{D}{r}\frac{c(i,j+1,k) - c(i,j,k)}{\Delta q} + \frac{N_A e}{RT} Dz \frac{E_q}{r} \frac{c(i,j+1,k) + c(i,j,k)}{2} \\
J_z(i, j, k+\tfrac{1}{2}) =& -D\frac{c(i,j,k+1) - c(i,j,k)}{\Delta z} + \frac{N_A e}{RT} DzE_z \frac{c(i,j,k+1) + c(i,j,k)}{2}.
\end{aligned}
\tag{15}
$$

III.   METHOD

In this project a cylindrical coordinate PNP equation numerical solver is implemented. The code is written in Matlab. The grid cell size is set to 0.2 nm to properly resolve the the surface structure. The time step is set to 1 ps to maximize simulation speed while ensuring simulation stability. In this project, the cell domain of interest is modeled as a hexagonal prism model in the cylindrical-coordinate system. To transform from a 2-D Cartesian (x, y) system to a 3-D cylindrical (r, z, ϕ) system, one can first switch from (x, y) to (r, t) for every single "slice" of the simulation domain. FIG. 2(a) shows the side view of the simulation domain, where one can find that is equivalent to an (x, y) grid. The third orthogonal axis in the cylindrical coordinate is the angle about the central z axis, denoted as q. In this report, While in a circularly symmetric system, everything should be independent of the angle q, here q-dependent variables, e.g. E_q and J_q, are still explicitly calculated and kept track of for generality. Later their values will be examined, which should be all zeros.

FIG. 2(b) shows the geometry arrangement of concentration and flux profiles in a wedge-shaped cell. Grid of concentration is equally spaced along r and z axis, as shown in FIG. 2(a), and is spaced by rdq, where r is the position along the radial direction and dq is the angular
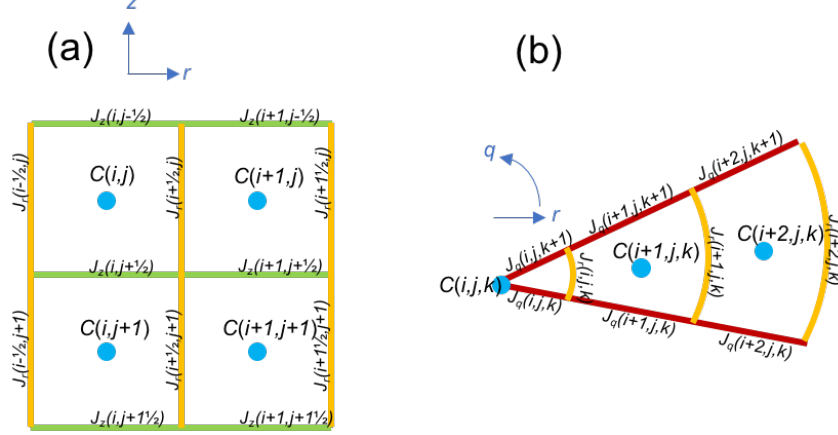
FIG. 2. (a) Arrangement of grids of concentration c and flux J_r and J_z profiles in a side view. Electric field E_r and E_z has the same grid location as J_r and J_z, respectively. (b) Arrangement of grids in a wedged cell in a top view.

spacing in the cylindrical coordinate. In this work, $dq = 0.5$ degrees is chosen to ensure the resolution at the outermost r ring is still fine enough.

To depict the edge of a hexagonal tile, the position of the boundary along r is modeled as a function of azimuth angle q. Specifically, as shown in FIG. 3, the distance between the side of the hexagon and the center, denoted B, is a function of q, and is within the range of $[\frac{\sqrt{3}}{2}C, C]$. In other words, when angle $\alpha = 0°$, the distance is C, i.e. the circumradius of the hexagon, while when $\alpha = 30°$, $B = \frac{\sqrt{3}}{2}C$. Using the law of singes, B can be mathematically formulated as

$$B = C\frac{\sin 60°}{\sin(180° - 60° - \alpha)}, 0° \leq \alpha \leq 60°. \tag{16}$$

Once this distance between the center and the side is known, a BC, e.g. periodic or Nuemann, can be placed accordingly.

Based on [4], the simulation domain is set to 40 nm (200 px) in height, 11.1 nm (56 px) in radius. The S-layer is place at the center of the domain, i.e. $z = 20$ nm. A pore of radius 1.3 nm that allows ions to pass is placed at the center of the S-layer. The surface density of the negative charges on the S-layer is $0.004e^-$ per nm^2. The reaction rate is 10 per second. Bulk concentration of NH$_4^+$ is set to 10 nM, as literature suggests that AOA can survive in an environment whose ammonia/ammonium concentration is below detection limit.
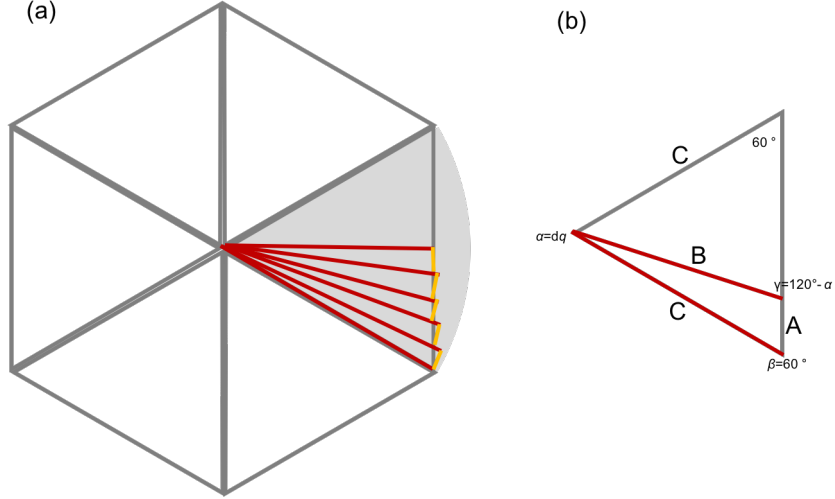
FIG. 3. (a) The hexagonal symmetry model is built on top of the cylindrical coordinate, therefore the distance between the hexagon side and the central axis is represented as a function of angular coordinate q. (b) The length of B can be calculated by using the law of sines.

IV. RESULTS

A. Fick solver

The model is first tested with the Fick's laws equation, which were introduced in Sec. II A. FIG. 4 shows the simulation results of the Fick solver. FIG. 4(a,b) show a concentration dip at $z = 30$ nm, demonstrating the implemented Fick diffusion-reaction solver worked as expected. FIG. 4(f) shows the convergence of the simulation, which is defined as

$$\text{convg} = \frac{\sum_{i,j} |c_{i,j}^{(t)} - c_{i,j}^{(t-1)}|}{\sum_{i,j} c_{i,j}^{(t)}}, \tag{17}$$

where (t) denotes the time-step number.

B. PNP solver

FIG. 5 shows the simulation results of the PNP solver. As shown in FIG. 5(a) and (b), it is the notable that surface charges on the S-layer greatly elevate the concentration level by a factor of 10^7, especially in the setting of very low bulk concentration, where the Debye length extends to the scale of micronmeters [7].

8
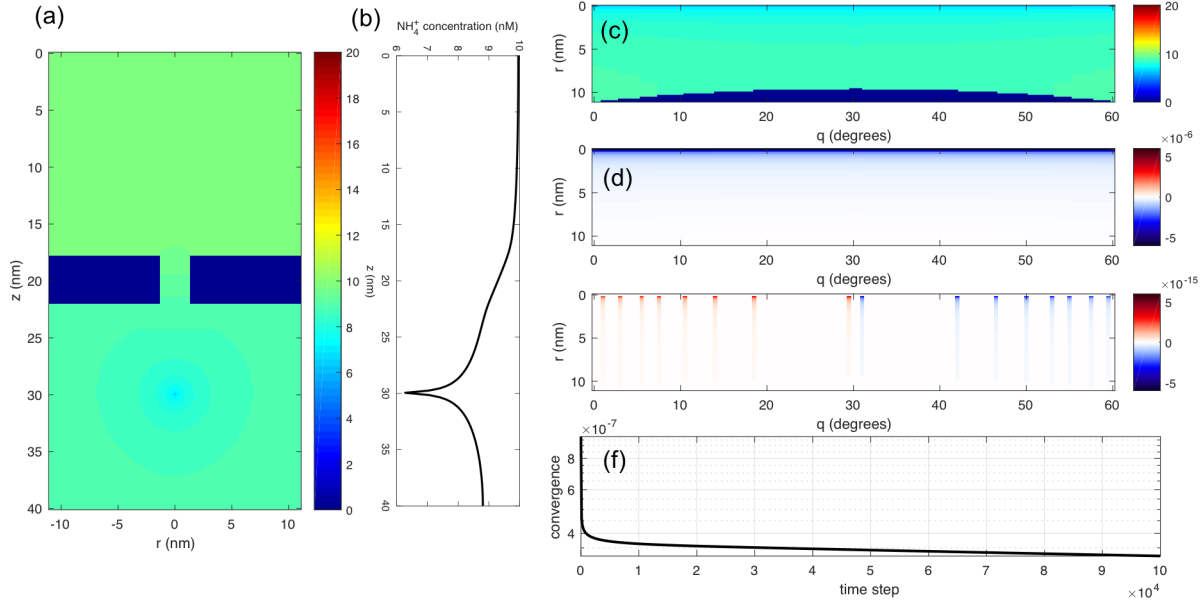
FIG. 4. Simulation result of the Fick solver. (a) Concentration profile map at the slice $q = 0°$. (b) Concentration profile along z at $r = 0$. (c) Concentration profile as a r-q map at $z = 30$ nm. (d) Radial flux J_r and (e) azimuthal flux J_q profile at $z = 30$ nm (arbitrary units). (f) Convergence vs. time step.

V. DISCUSSION

In Sec. III, it was predicted that the J_q component should be all zeros. However, FIG. 4(f) and FIG. 5 both show very weird patterns, indicating that the previous prediction is not true. A way to account for these non-zero values is that these values are due to numerical error and are hence negligible, which is true, as they are 9 orders of magnitude smaller than their J_r or J_z counterparts.

An intriguing aspect which was not investigated in this report is that, our implementation of hexagonal boundary condition might require a certain azimuthal cell resolution. Theoretically, the higher spatial resolution would give better result, but also require more computation resources. In fact, the time complexity is $O((\Delta)^{-4})$, as the azimuthal grid size dq and time step size Δ also depend on the Cartesian grid size Δx. Therefore, another way to look at this problem would be: what is the maximal Δ that the proposed hexagonal BC scheme would still work.

9
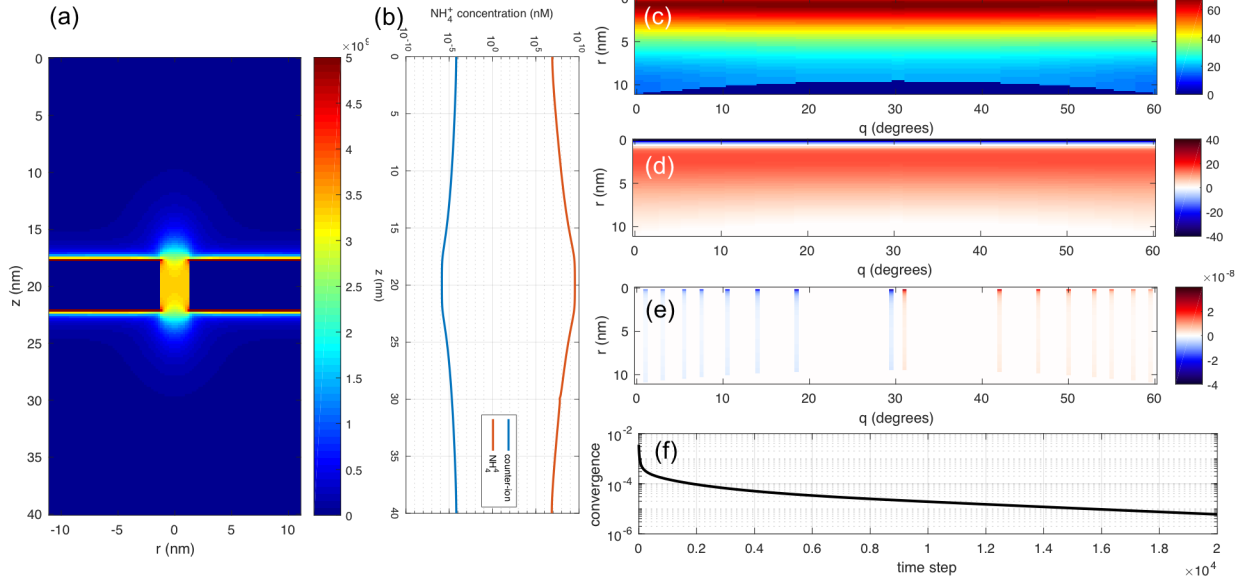
FIG. 5. Simulation result of the PNP solver. (a) NH_4^+ concentration profile map at the slice $q = 0°$. (b) NH_4^+ and the counter-ion concentration profile along z at $r = 0$. (c) NH_4^+ concentration profile as a r-q map at $z = 30$ nm. (d) NH_4^+ radial flux J_r and (e) azimuthal flux J_q profile at $z = 30$ nm (arbitrary units). (f) Convergence vs. time step.

VI. SUMMARY

To sum up, in this project I implemented a 3-D diffusion-reaction model which is specialized for hexagonal structure. Using AOA as an example, I studied the transport behavior of NH_4^+ ions in a non-charged setting with a Fick's equations solver and a PNP equations solver. The implemented model allows the study of a 3-D model at very low computation cost thanks to the symmetry of the model domain.

[1] U.B. Sleytr *et al.* "S-layers: principles and applications," FEMS Microbiol. Rev. **38**, 823 (2014).

[2] J. Herrmann *et al.* , "Environmental Calcium controls alternate physical states of the Caulobacter surface layer," Biophys. J. **112**, 1841 (2017).

[3] M.A. Arbing *et al.* , "Structure of the surface layer of the methanogenic archaean Methanosarcina acetivorans," **109**, 11812 (2012).

[4] P. Li *et al.* , "Electron cryo-tomography and reaction-diffusion simulations reveal an evolutionary basis for charged archaeal surface layer proteins," submitted.

[5] D.A. Stahl, "Physiology and Diversity of Ammonia-Oxidizing Archaea," Annu. Rev. Microbiol. **66** 83 (2012).

[6] J.J. Jasielec, "Computer simulations of electrodiffusion problems based on NernstPlanck and Poisson equations," Comput. Mater. Sci. **63**, 75 (2012).

[7] D. Andelman, "Introduction to Electrostatics in Soft and Biological Matter," (2004).